The EMBO Journal vol.15 no.11 pp.2858–2869, 1996

Developmentally programmed DNA deletion in *Tetrahymena thermophila* by a transposition-like reaction pathway

Sergei V.Saveliev and Michael M.Cox[1]

Department of Biochemistry, College of Agriculture and Life Sciences, University of Wisconsin, Madison, WI 53706, USA

[1]Corresponding author

We provide a molecular description of key intermediates in the deletion of two internal eliminated sequences (IES elements), the M and R regions, during macronuclear development in *Tetrahymena thermophila*. Using a variety of PCR-based methods *in vivo*, double-strand breaks are detected that are generated by hydrolytic cleavage and correspond closely to the observed chromosomal junctions left behind in the macronuclei. The breaks exhibit a temporal and structural relationship to the deletion reaction that provides strong evidence that they are intermediates in the deletion pathway. Breaks in the individual strands are staggered by 4 bp, producing a four nucleotide 5′ extension. Evidence is presented that breaks do not occur simultaneously at both ends. The results are most consistent with a deletion mechanism featuring initiation by double-strand cleavage at one end of the deleted element, followed by transesterification to generate the macronuclear junction on one DNA strand. An adenosine residue is found at all the nucleophilic 3′ ends used in the postulated transesterification step. Evidence for the transesterification step is provided by detection of a 3′ hydroxyl that would be liberated by such a step at a deletion boundary where no other DNA strand ends are detected.

Keywords: ciliated protozoa/DNA cleavage/DNA deletion/DNA recombination/polymerase chain reaction

Introduction

Tetrahymena thermophila is a binuclear ciliated protozoan. The diploid micronucleus is transcriptionally inactive and is an analog of an inactive germ cell nucleus. The polyploid macronucleus is responsible for all gene expression in the organism. During conjugation, the sexual phase of the ciliate life cycle, the conjugants exchange haploid gametic nuclei to form diploid zygotic nuclei. The old macronucleus is destroyed and a new one is developed from a copy of the zygotic diploid nucleus (Orias, 1986). Extensive programmed genome rearrangements occur during macronuclear development. These include breakage of chromosomes into smaller fragments (Yao, 1989), which are then converted into small chromosomes by the addition of telomeres (Blackburn, 1992). Each of the small chromosomes is amplified in number ~50-fold during macronuclear development. In addition, ~15% of the *Tetrahymena* micronuclear genome is eliminated in the form of >6000 site-specific deletions. The eliminated sequences are of different types, collectively referred to as internal eliminated sequences (IES elements). Some IES elements, including most of those identified to date in hypotrichous ciliates, fall into identifiable families of transposon-like sequences (Cherry and Blackburn, 1985; Jaraczewski and Jahn, 1993; Klobutcher *et al.*, 1993; Williams *et al.*, 1993; Doak *et al.*, 1994; Wells *et al.*, 1994; Klobutcher and Herrick, 1995). In *Tetrahymena*, a holotrichous ciliate, the majority of the deleted sequence elements characterized to date are relatively heterogeneous and short (a few kilobase pairs or less), and display little obvious relationship to transposons in their sequence structure (Yao, 1989; Katoh *et al.*, 1993; Heinonen and Pearlman, 1994). The entire conjugation process in *Tetrahymena* is complete in ~20 h (Martindale, *et al.*, 1982), with the DNA deletions occurring efficiently within a 2 h period commencing ~10–12 h after conjugation initiates (Austerberry *et al.*, 1984).

Two IES elements in *Tetrahymena*, designated the M and R regions (Figure 1), have been particularly well characterized by Yao and co-workers (Austerberry and Yao, 1987, 1988; Godiska and Yao, 1990; Godiska *et al.*, 1993). In the M region, two alternative deletions of either 600 or 900 bp are observed, sharing their right boundary. In the R region there is a single deletion of 1.1 kbp. There is some microheterogeneity in the observed chromosomal junctions left behind by deletion, with two or three alternative sets of deletion endpoints for each of these IES elements (Austerberry *et al.*, 1989; Saveliev and Cox, 1994). The alternative endpoints are generally found within a few base pairs of each other. M region deletions are directed largely by a *cis*-acting polypurine tract (G_5) found 41–54 bp distal to each deletion endpoint (Godiska and Yao, 1990; Godiska *et al.*, 1993). Short repeats found at some of the deletion boundaries have no demonstrated function in the deletion process.

Very little is known about the mechanism of these developmentally programmed deletion reactions or about the enzymes that promote them. In hypotrichs, the Tec and other IES elements of *Euplotes crassus* (Jaraczewski and Jahn, 1993; Klobutcher *et al.*, 1993) and the TBE1 elements of *Oxytricha trifallax* (Williams *et al.*, 1993) are eliminated as circular DNA molecules. The structures of the circle junctions where the element ends are joined suggested that *Euplotes* elements were excised in a pathway initiated with double-strand breaks at both ends, followed by annealing and repair of the ends to give the deleted circle (Jaraczewski and Jahn, 1993; Klobutcher *et al.*, 1993). A transposition-like mechanism was suggested for the excision of TBE1 elements, initiated with a double-strand break on only one element end (Williams *et al.*, 1993). In contrast, the deleted DNA in the M and R regions of *Tetrahymena* is generally released as a linear

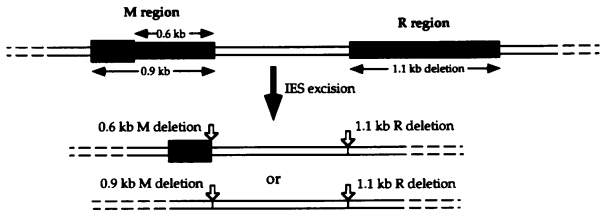

Fig. 1. IES excision in the M and R regions. In the M region, the two different deletions of 0.6 and 0.9 kb are observed. These share a common right boundary. IES elements are designated by filled boxes. Open arrows are chromosomal junctions left by excised IESs.

DNA molecule (Saveliev and Cox, 1994; Yao and Yao, 1994), suggesting that the M and R region deletions are mechanistically distinct in at least some respects from those observed to date in the hypotrichs. This could reflect a more general mechanistic and enzymatic dichotomy in the deletion reactions observed in hypotrichs and holotrichs. The only protein implicated to date in the deletion reactions is the p65 protein of *Tetrahymena*, which appears to be associated with specialized vesicles in which the deleted DNA is processed or degraded (Madireddi *et al.*, 1994).

Some potential intermediates in the deletion of the M and R regions have been characterized. Using ligation-mediated PCR, DNA strand breaks have been detected *in vivo* at the ends of the M and R regions (Saveliev and Cox, 1995). The breaks occur only during the DNA rearrangement period of macronuclear development, and their locations correspond closely with the known chromosomal junctions left behind in the mature macronucleus. They appear on both DNA strands, staggered by 4 bp, and the 5′ ends are phosphorylated (Saveliev and Cox, 1995). In 11 of 12 cases, the 3′-terminal residue at a break was an adenosine. Collectively, the results suggested that the deletion process was initiated by a double-strand break at one end of the element, followed by direct nucleophilic attack of the exposed 3′ hydroxyl group on the phosphodiester bond at the other end of the element. This pathway is transposition-like in that it employs a direct transesterification step involving different segments of DNA.

However, the earlier study could not eliminate several alternative reaction pathways, particularly those in which deletion is initiated by breaks at both element ends. In addition, many features of the model remain untested. Instead of the hydrolytic cleavage proposed by the model, the initiating break could be generated by attack of an amino acid side chain (e.g. tyrosine or serine) on a phosphodiester bond to form a transient covalent 3′ DNA linkage to the protein, as in the case of many site-specific recombinases and topoisomerases (Craig, 1988). There should be 3′ hydroxyl groups at the strand break sites only in the case of a hydrolytic cleavage. The initiating breaks could also occur only on one DNA strand, instead of simultaneously on both strands to generate a double-strand break. Here, this deletion pathway is refined and major predictions of the model are tested *in vivo*. As part of this effort, we complete the molecular description of the structure of DNA breaks at the M and R region boundaries, and provide new evidence that these are intermediates in the deletion pathway.

Results

Experimental design

As is the case with other ciliates, the sexual cycle of *T.thermophila* can be synchronized. By simply mixing the pre-starved cells of two different mating types, virtually the entire culture can be induced to initiate conjugation. The programmed genomic DNA deletions associated with macronuclear development commence 10–12 h after the initiation of a synchronized conjugation. Genomic DNA extracted from these cells should be enriched for the intermediates produced in the deletion reactions.

Free DNA ends are expected to appear as DNA deletion reaction intermediates in the conjugating cells, either as a result of DNA cleavage to initiate the deletion process or as products of subsequent steps. The ends can be detected and characterized by PCR-based methods in a number of variations. Synchronization of conjugation ensures the presentation of ends at sufficiently high levels in the cell lysates to distinguish them from the random DNA ends produced in other cellular DNA processes or as a result of DNA breakage during preparation of the cell lysate for analysis.

Strand breaks were detected by ligation-mediated PCR in an earlier study (Saveliev and Cox, 1995), using a protocol that allowed structural characterization of only the free 5′ end at the site of the break. The work described below was designed to define the structure of the DNA ends created transiently by the deletion process and test additional predictions of the model outlined in the Introduction. All of the experiments involve PCR protocols in which the first step involves the attachment of a linker or extension to the DNA end being analyzed. Cleavage at the boundaries of the deleted element produces DNA ends on either side of the cleavage site. The ends reflecting DNA retained in the mature macronucleus or DNA deleted as part of the IES element are referred to below as MAC and MIC ends, respectively.

Detection of free 3′ DNA ends

If the DNA strand breaks associated with the DNA deletion events (Saveliev and Cox, 1995) are produced via simple hydrolytic cleavage, the resulting 3′ DNA ends would have free hydroxyl groups. A 3′ end with this structure would be labeled with terminal deoxynucleotidyl transferase (TdT) to produce long deoxynucleotide homopolymeric tails (Deng and Wu, 1983). The labeled ends can then be recovered with the anchored PCR procedure (Loh *et al.*, 1989), as outlined in Figure 2A.

We labeled the 3′ DNA ends with poly(dG) tails, because previous reports showed that TdT synthesizes poly(dG) tails which are relatively short and homogenous (between 30 and 50 bp in a length) (Deng and Wu, 1983). We anticipated that the use of a relatively homogenous set of poly(dG) tails would lead to generation of more homogenous PCR products and simplify analysis. Because the *Tetrahymena* genome is very AT-rich, the use of poly(dG) also minimizes the chances of ambiguity about where the genomic sequences end and the TdT-generated tail begins. Separate primer sets were designed to characterize the MAC and MIC ends at each deletion boundary. As described in Materials and methods and in the previous report (Saveliev and Cox, 1995), special precautions were

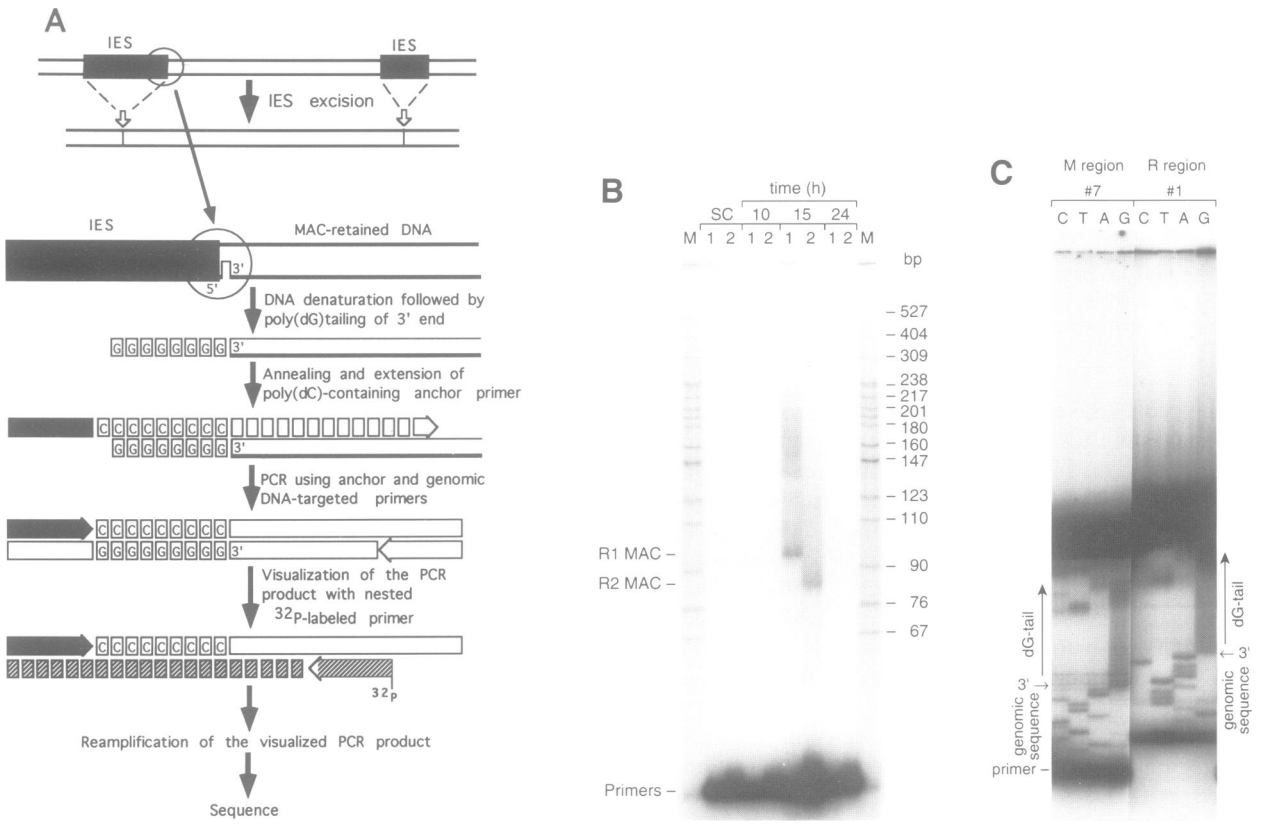

Fig. 2. Detection of breaks with free 3′ hydroxyl groups at the boundaries of the M and R regions. (**A**) PCR protocol to detect free 3′ DNA ends in a cell lysate. DNA cleavage leaves a transient break at an IES boundary. Rapid lysis of the cells preserves the break in the genomic DNA. The DNA is denatured to expose free 3′ hydroxyl. The end is extended to generate a poly(dG) tail in a terminal deoxynucleotidyl transferase-mediated reaction. The end is recovered in subsequent PCR steps using a poly(dC)-containing anchor oligonucleotide and a primer targeted to the genomic DNA near the anticipated break. Visualization of the PCR product involves extension of a ^{32}P-labeled nested primer. After reamplification, the PCR product is sequenced to define the position of the 3′ end. (**B**) Detection of the free 3′ DNA ends at the R region boundaries. The figure represents visualized PCR products obtained during analysis of the MAC 3′ ends at boundaries R1 and R2 (lanes designated 1 and 2, respectively). Cell lysates were analyzed at different times after initiation of conjugation. Starved cells (SC) were used as a control. The molecular size markers (lane M) are pBR322 fragments generated by *Msp*I digestion. (**C**) Sequencing analysis of the PCR products. The genomic 3′ end occurs at the position defined by the end of the poly(dG) tail. The analyzed ends are identified by numbers at the top of the sequencing lanes, which correspond to the numbers at each end in Figure 4.

necessary to avoid non-specific breakage of the genomic DNA during isolation and thereby reduce the non-specific background in these procedures.

A temporal screen of conjugating cultures detected prominent PCR products 15 h after conjugation was initiated (Figure 2B). No specific signal was detected at other times examined or in starved cells prior to conjugation (Figure 2B). The PCR products appeared as smears, an expected consequence of the length variability of the PCR products that is inherent in the procedure. The shortest PCR molecules in each smear precisely map the corresponding 3′ DNA end. The size of the smear varied, spanning 30–100 bp or more in different trials, indicating a greater variability in the TdT step than we had anticipated. This had little effect on results, since the protocol used to sequence the amplified ends is unaffected by the length of the poly(dG) tail.

We found 3′ DNA ends with free hydroxyl groups at every element end where we had previously found DNA strand breaks at the deletion boundaries. Some ends were recovered directly after the first PCR amplification. However, most of the ends required a second amplification with a nested chromosomal primer. This is in contrast to the 5′ end detection method used previously (Saveliev and Cox, 1995), and reflects the lower specificity of the first step of the procedure for 3′ end-labeling with TdT. TdT will label all free 3′ hydroxyl groups available. The oligonucleotide linker and primer sequences and other features of the PCR methods were empirically adjusted to optimize the yield of the specific PCR products. The dilution factors between PCR amplifications and the extension times during each PCR cycle were found to be particularly critical parameters.

The free 3′ DNA ends map to positions defined by the IES boundaries

The PCR products were sequenced to define each 3′ DNA end. Because of the heterogeneous population of PCR products (the smear) generated by the protocol, we sequenced DNA from different zones of the smear to prove that all the PCR molecules are products of amplification of the same 3′ DNA end. Each zone contained the same genomic sequence followed by a poly(dG) tail of different length. Figure 2C shows a typical sequencing analysis of one zone from two different ends. Each 3′ end was detected and sequenced in at least two independent experiments using lysate preparations from at least two different

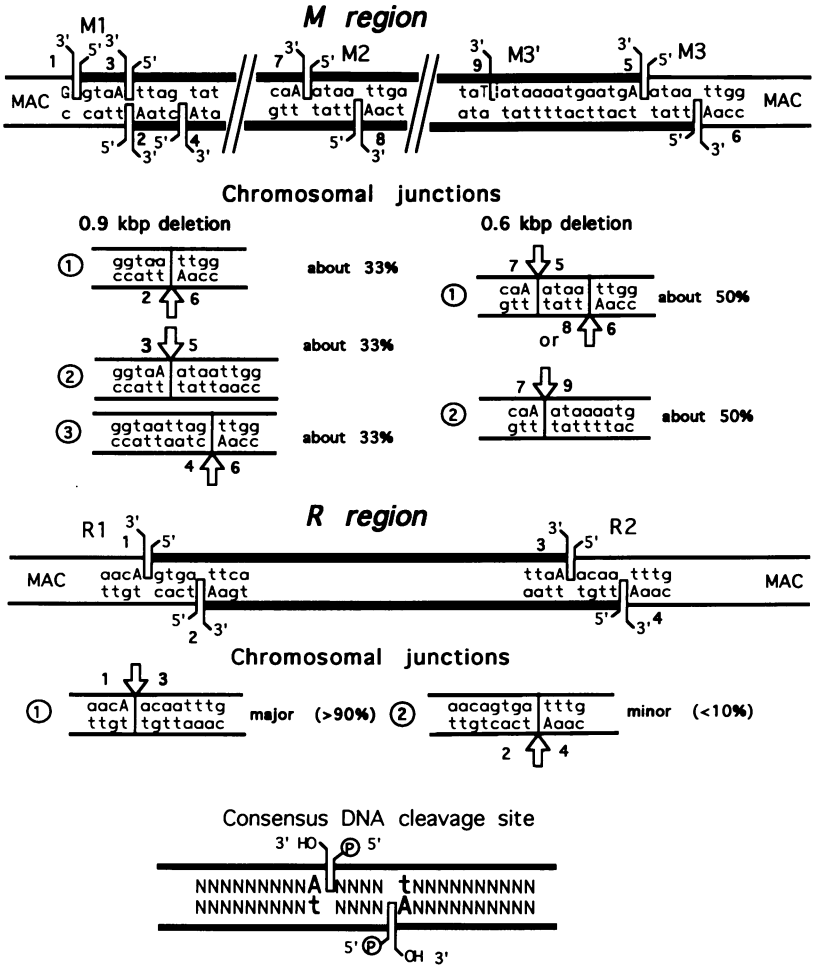

Fig. 3. Summary of DNA ends appearing at the boundaries of the M and R regions during macronuclear development in *T.thermophila*. Deletion boundaries are labeled M1, M2, R1, etc. Observed breaks are numbered separately for the two regions (e.g. the breaks at boundary M1 are numbered 1–4). The 5′ ends shown are from Saveliev and Cox (1995). The 3′ ends depicted are those defined in this study. The chromosomal junctions left behind by deletions are indicated by open arrows, flanked by the numbers of the ends presumably brought together at the junction. The approximate representation of each macronuclear chromosomal junction among those detected for the indicated deletion is indicated by the percentages shown near each junction. A consensus DNA cleavage site is shown at the bottom, detailing the chemical structure of the breaks. The 3′ hydroxyl and 5′ phosphate groups are designated as OH or a circled P, respectively. Only the conserved residues flanking the cleavage sites are shown. Within the M region, a number of the 4 bp between the cleavage sites are also conserved. In particular, the central two residues are all 5′ TA. We do not know if this identity is significant, and it does not appear in the R region ends.

cultures of conjugating cells. Each end always appeared at the same position.

All the 3′ ends appeared at the precise positions of the DNA strand breaks defined earlier in the study of free 5′ DNA ends (Figure 3). On any one strand, the ends defined in Figure 3 can be joined to create one or more of the observed chromosomal junctions. Because the breaks are staggered by 4 bp on the complementary strands, joining of the ends on different strands results in two slightly different chromosomal junctions, which are shifted by 4 bp relative to each other. The limited microheterogeneity observed in the chromosomal junctions in mature macronuclei can be explained by viewing the joining of observed MAC ends on one strand or the other as alternative outcomes. In the R region, for example, joining of the MAC ends at breaks 1 and 3 on the upper strand corresponds to chromosomal junction 1, and joining the MAC ends at the breaks 2 and 4 on the bottom strand generates chromosomal junction 2 (Figure 3).

The M region ends at M1 and M3 were special cases. At M1, there were two alternative break sites detected on each complementary strand (Figure 3, M region breaks 1–4), separated in each case by four nucleotides. The breaks were found in a close examination of the sequencing data. PCR products obtained during amplification of the tailed DNA from each of the two 3′ ends merged into one general smear. The sequence of the total product, however, revealed a 4 bp region in which two sequences overlapped immediately adjacent to the poly(dG) tail (data not shown). The short overlapping sequences were consistent with a pair of 3′ ends on each strand in the locations corresponding precisely with the 5′ ends defined earlier (Saveliev and Cox, 1995).

Based on microheterogeneity in chromosomal junctions characterized in mature macronuclei, there are two predicted alternative boundaries on the right side of the 0.6 kbp deletion in the M region, designated M3 and M3′ (Austerberry and Yao, 1988; Saveliev and Cox, 1994) and separated by 13 bp. Both are used for deletion at approximately equal frequency. We previously found that

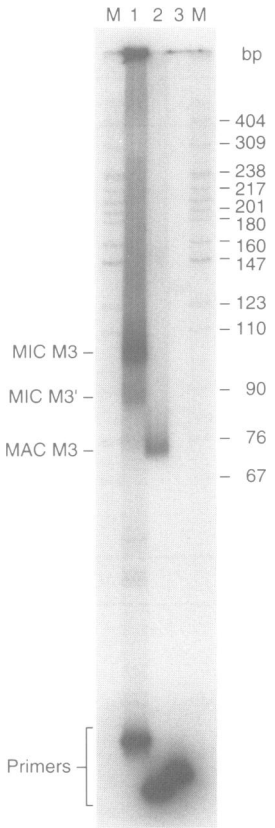

Fig. 4. A transient exposed 3′ end on the MIC side of the M3′ boundary. MIC M3 and MIC M3′ designate PCR products resulting from amplification of free MIC ends at M3 and M3′, respectively (lane 1). Lanes 2 and 3 show trials to detect 3′ ends on the MAC side of M3 and M3′, or M3′ alone, respectively. MAC M3 designates the free 3′ end found on the MAC side of M3 (lane 2). The PCR products observed for the MAC 3′ ends were visualized with M3MACvis (lane 2) and M3MACvis2 (lane 3) primers. The M3MACvis2 primer spans M3 and would permit visualization of the PCR product resulting from amplification of a 3′ end at M3′ only. The molecular size markers (lanes M) are pBR322 fragments generated by *Msp*I digestion.

DNA strand breaks appear at only the M3 boundary (Saveliev and Cox, 1995). The absence of the DNA breaks at the M3′ boundary was treated as evidence that DNA cleavage to initiate deletion never occurs at M3′. If deletion is initiated with a double-strand break at M2, followed by attack of the free 3′ hydroxyl group on the phosphodiester bond at M3′, the resulting trans-esterification should produce a free 3′ end on the MIC side of M3′ without a corresponding 5′ phosphate at the same location. The MIC 3′ ends at M3 and M3′ were analyzed therefore as shown in Figure 4. In lane 1, two smears are evident, with the upper one shifted by 13 bp relative to the lower one. Sequence analysis on the lower smear showed that it arose from amplification of DNA with a tailed 3′ end precisely at M3′ (Figure 3, break 9). The upper smear defines the M3 boundary. The end at M3′ gives a weaker signal than M3, consistent with the fact that M3′ is a potential boundary only for the 0.6 kbp deletions, while M3 serves as a boundary for both 0.9 and 0.6 kbp deletions.

The MAC 3′ ends (on the opposite strand) were also analyzed at the M3 and M3′ boundaries. A single end was detected (Figure 4, lane 2), and sequencing analysis showed that it corresponded to the M3 boundary (Figure 3, 3′ end at break 6). Since efficient cleavage at M3 might obscure a DNA end at M3′ in this experiment, we used the M3MACVis2 primer (which spans M3) for the final visualization step to detect uniquely any breaks that might occur at M3′. No PCR product was detected on the MAC side of M3′ (Figure 4, lane 3) in seven separate trials with two different lysate preparations. To determine if a 3′ end was labeled at an efficiency too low to be visualized, the corresponding zone was cut out of the gel and a PCR amplification was carried out on the extracted material. Sequencing analysis did not reveal any specific 3′ ends at M3′ in the reamplified product. The apparent absence of a free 3′ end on the MAC side of M3′ is consistent with the idea that cleavage does not occur at M3′ to initiate deletion.

DNA cleavage at the deletion boundaries produces double-strand breaks with four nucleotide 5′ extensions

The consensus structure of the DNA strand breaks is shown in Figure 3. Wherever a strand break in which both the 3′ and 5′ ends have been detected and characterized occurs at a deletion boundary, a similar break appears on the complementary strand but staggered by 4 bp. We wished to determine if both strands were cleaved simultaneously, producing double-strand breaks with the structure shown. The breaks characterized above provide a guide for the design of linkers compatible with the predicted open DNA ends possessing a four nucleotide 5′ extension.

The method used to detect each double-strand break (Figure 5A) is specific for the end expected to be generated, and proved to be more sensitive and straightforward than the methods used to characterize the individual 5′ and 3′ ends at the breaks. A strong signal corresponding to double-strand breaks at the deletion boundaries appeared at 15 h of conjugation, during the DNA rearrangement period (Figure 5B). At each deletion boundary, we detected open chromosomal ends on both the MIC and MAC sides of each break characterized, with the results summarized in Figure 6. In multiple trials with each set of linkers and primers, no signals were detected in starved cells, at 10 h into the conjugation process (immediately prior to the DNA rearrangement period), and at 24 h. This again demonstrated that the breaks are related temporally to the DNA deletion process. Very strong signals with relatively little background were obtained with as little as 15 ng of the total genomic DNA in these trials, and the PCR products were visualized readily after one amplification. For comparison, the protocols used to characterize the 5′ and 3′ ends required 100 ng or more of total genomic DNA.

The boundaries at M1 and M3′ again provided exceptions to the general pattern. As might be expected from the data in Figure 3, two different double-strand breaks (both MIC and MAC ends) were found at the M1 deletion boundary. The ends result from alternative DNA cleavages defined by breaks 1 and 2 at the outer cleavage site and by breaks 3 and 4 at the inner cleavage site (Figures 3 and 6). Also as expected, a strong double-strand break signal appeared for the M3 boundary but not at M3′ (Figure 7). In multiple independent trials with two lysate

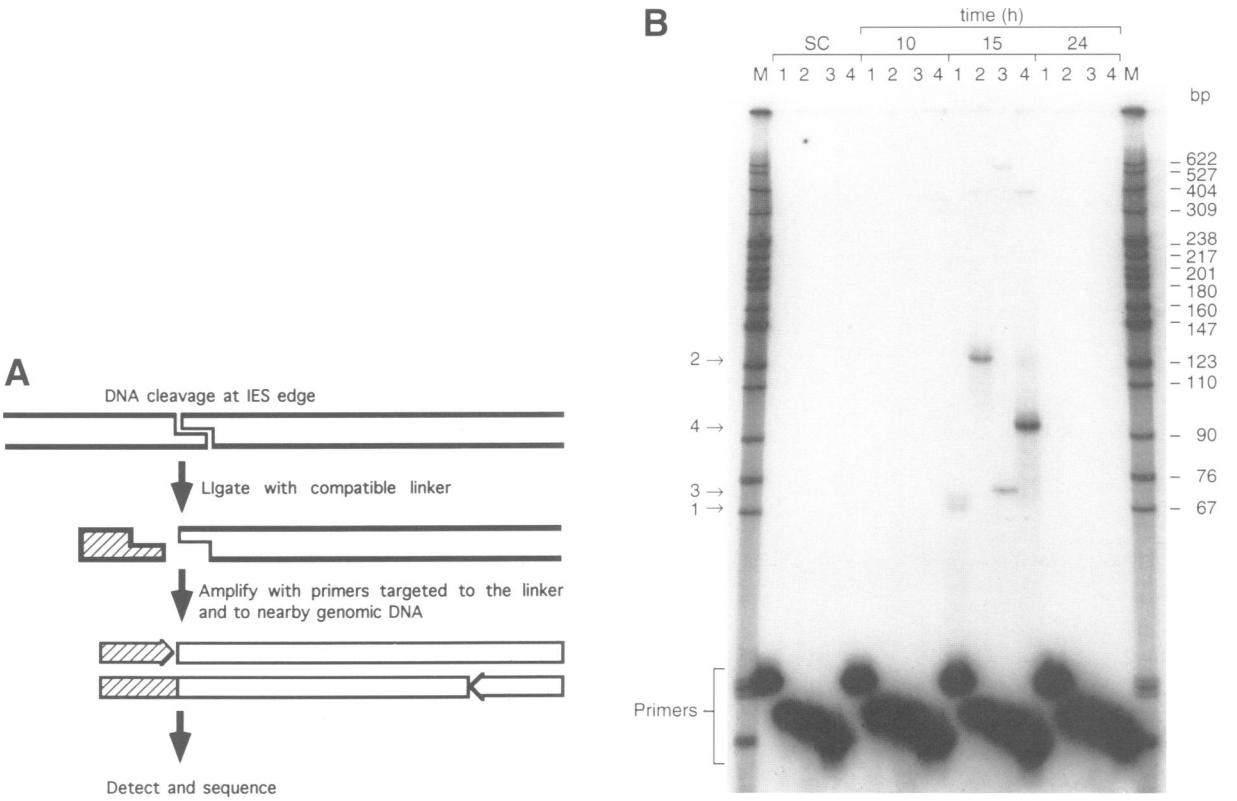

Fig. 5. Double-strand breaks are detected at IES boundaries. (**A**) Ligation-mediated PCR approach used to detect double-stranded breaks with the general structure shown in Figure 3. If both DNA strands are cut during IES excision, the open ends can be detected by ligation with compatible linkers. The ligated ends are then recovered by PCR using one oligonucleotide primer targeted to the linker and another primer targeted to nearby genomic DNA. Steps to visualize and sequence the PCR products are the same as those for 3′ end detection (Figure 3A). (**B**) Detection of double-stranded breaks. Cell lysates were analyzed at different times in hours (h) after initiation of conjugation. SC denotes starved cells. Detected chromosomal ends shown were at the MAC and MIC sides of R2 (lanes and bands labeled 1 and 2, respectively) and M2 (lanes and bands labeled 3 and 4, respectively). Bands associated with IES ends are distinguished from non-specific background by size and by direct sequencing as described in the text. The molecular size markers (lane M) are pBR322 fragments generated by *Msp*I digestion.

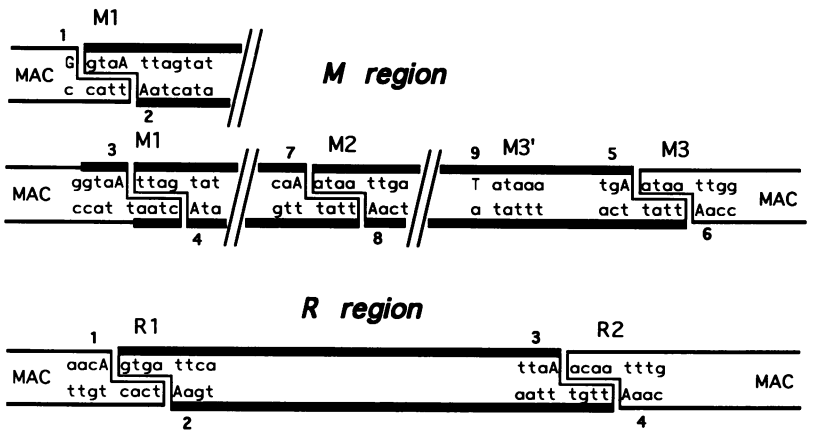

Fig. 6. Map of double-stranded breaks detected in this study. Reciprocal open ends on the MIC and MAC sides of each break shown were detected and characterized in each case. Additional designations and symbols are as in Figure 3.

preparations (10 and six trials for the MIC and MAC ends, respectively), no signal above the non-specific background was detected at M3′. Low level non-specific background signals were generated in many experiments, presumably originating from breakdown of the old macronuclear DNA or degradation of the released deleted sequences in the developing macronucleus. However, these did not obscure the specific signals corresponding to the deletion boundaries.

We tried to assess further the specificity of the procedure used to analyze double-strand breaks, addressing in particular the remote possibility that the double-stranded linkers could be ligated to breaks occurring on only one strand, or to double-strand breaks with a structure other

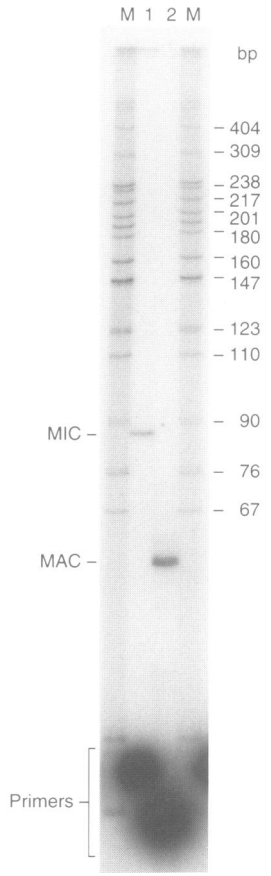

Fig. 7. Open double-stranded DNA ends appear at M3, but not M3′, during a 0.6 kbp excision in the M region. MIC and MAC denote the PCR products resulting from amplification of open MIC and MAC ends at M3 (lanes 1 and 2, respectively). In this instance, the linkers used to detect the ends at M3 are also compatible with the cleavage expected at M3′ if one were to occur. The molecular size markers (lanes M) are pBR322 fragments generated by *Msp*I digestion.

than a four nucleotide 5′ extension. A set of linkers was generated analogous to those described above, but with five nucleotide 5′ extensions. If the linkers used in experiments such as those in Figure 5 could be ligated to DNA ends resulting from single-strand or non-specific double-strand breaks, linkers with five nucleotide 5′ extensions should be ligated just as well. The linkers would also detect specifically any minor 5 bp staggered breaks. The five nucleotide 5′ extensions on the linkers were designed to be complementary to the expected four nucleotide 5′ extension of the target plus one adjacent nucleotide. No specific signal comparable with those shown in Figure 5 was found at any deletion boundaries (data not shown). Minor PCR products of the expected length appeared in individual trials for two boundaries, but they did not prove to be reproducible. The results show that the method used to detect the double-strand breaks is highly specific and informative. As a minor footnote, the results provided evidence that ends with a five nucleotide 5′ extension complementary to the control linkers are not normally produced in the deletion pathway.

DNA cleavage does not occur simultaneously at both deletion boundaries

Although double-stranded breaks were detected at both ends of each deleted sequence element, the protocols described above were examining populations of molecules and do not demonstrate that both ends of a particular element are cleaved simultaneously. The lack of detectable breaks at the M3′ boundary suggested that deletion is initiated by a double-strand break at just one end to generate at least one of the observed junctions in macronuclear DNA. We therefore set out to determine if we could find elements in which a double-strand break had occurred at only one end. As shown above, detection of specific double-strand breaks based on direct ligation of complementary linkers is very sensitive. We therefore adapted this procedure by ligating the same linkers to the MIC ends at one end of an element and using the linker for one PCR amplification primer target as before. However, the second PCR amplification primer was targeted to sequences beyond the opposite end of the element, so that no PCR product would be obtained unless the opposite end of the element was intact (Figure 8A). Double-strand breaks detected in these experiments were termed initiating breaks and were tested for at all ends of the M and R regions.

In the first experiments, the PCR products obtained in this procedure were visualized with a primer which, like the amplification primer, was targeted to chromosomal DNA outside the deleted sequence. The visualized product was long (up to 1 kb), size resolution was relatively imprecise and the non-specific background was high (data not shown). To improve detection and resolution, new visualization primers were targeted to the micronucleus-specific DNA to generate a shorter product in the visualization step. However, there is a small possibility that PCR products might be amplified from deleted DNA sequence elements in which the specific linkers had somehow ligated to both ends, and subsequently detected by the MIC DNA-specific visualization primers. To eliminate this possible artifact, independent PCR amplifications were carried out using only the primer targeted to the ligated linkers. PCR products visualized with the MIC-specific visualization primers were never detected in these controls (data not shown).

The modified protocol permitted the detection of 'initiating breaks' in the M region (Figure 8B). The specific PCR products corresponding to the initiating breaks appeared during the DNA rearrangement period in conjugation and they were not detected during analysis of 10 and 24 h conjugating cells. We found the uncoupled initiating breaks at both boundaries of the 0.6 and 0.9 kbp deleted sequences in the M region, with results summarized in Figure 9. Initiating breaks were detected at all sites where there was an identified double-strand break, with the exception of the innermost of the two double-strand breaks at boundary M1, defined by DNA strand breaks 3 and 4 (Figures 3 and 6). An initiating break, as defined by the protocol described in Figure 8A, was not observed at this location in eight separate trials, even though the same protocol readily detects a break only 4 bp away at the site defined by strand breaks 1 and 2. As addressed in more detail below, the initiating break at strand breaks 1 and 2 is unique in the sense that cleavage here followed by transesterification would not yield any of the macronuclear junctions detected to date.

Trials to detect initiating breaks in the R region were not successful, perhaps because the DNA segment targeted

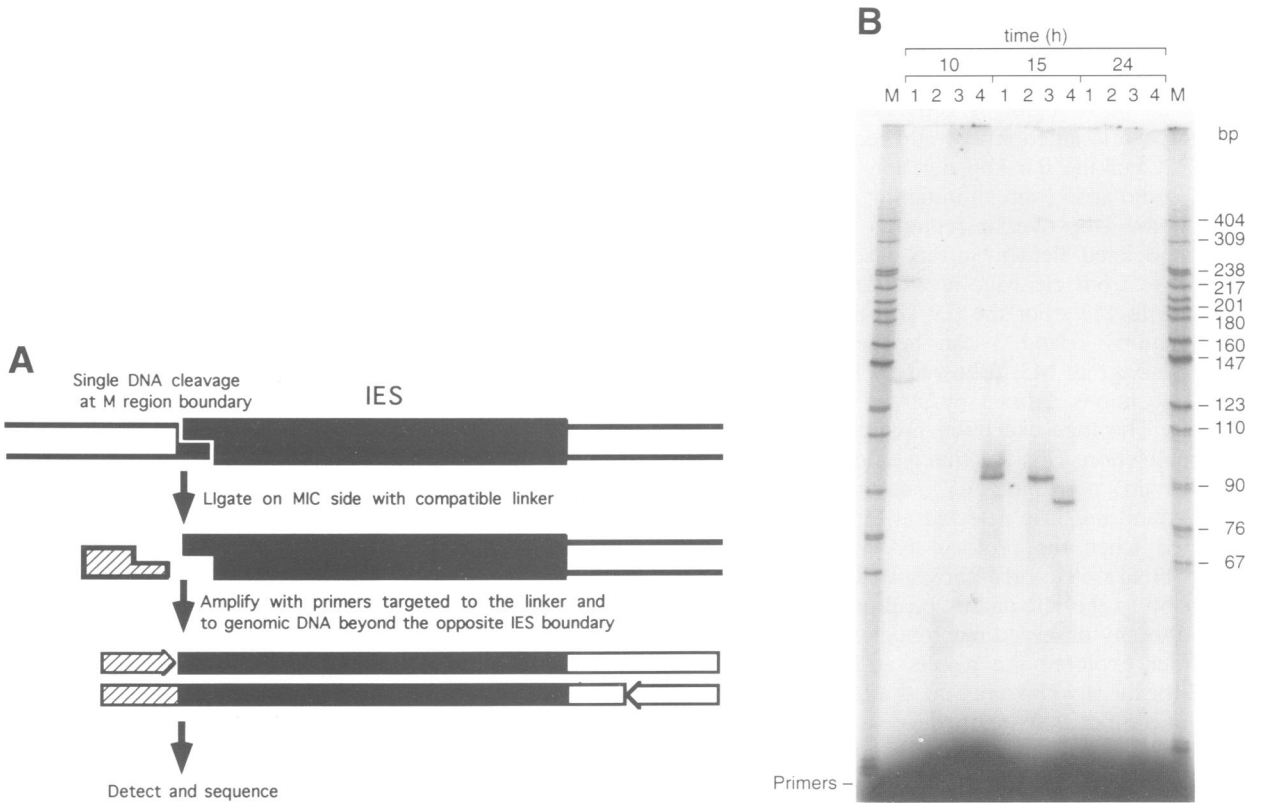

Fig. 8. Double-strand breaks need not occur simultaneously on both ends of an M region IES. (**A**) Technique to detect cleavage uniquely at one IES boundary. A linker compatible with the MIC side of the break to be analyzed is added and ligated. The ligated end is recovered by amplification with primers targeted to the linker and to MAC genomic sequences beyond the opposite IES boundary. No PCR product can be amplified unless the opposite IES boundary is intact. All symbols are as in Figure 5A. (**B**) Unique end cleavage in the M region. Genomic DNA was analyzed at different times after initiation of conjugation. Ends were detected with this protocol at the M1 site defined by DNA strand breaks 1 and 2 (lanes 1), at M2 (lanes 3) and at M3 (lanes 4). No unique end cleavage was detected at the alternative M1 site defined by strand breaks 3 and 4 (lanes 2), even though a double-strand break can be detected at this location by the protocol of Figure 5A. The molecular size markers (lane M) are pBR322 fragments generated by *Msp*I digestion.

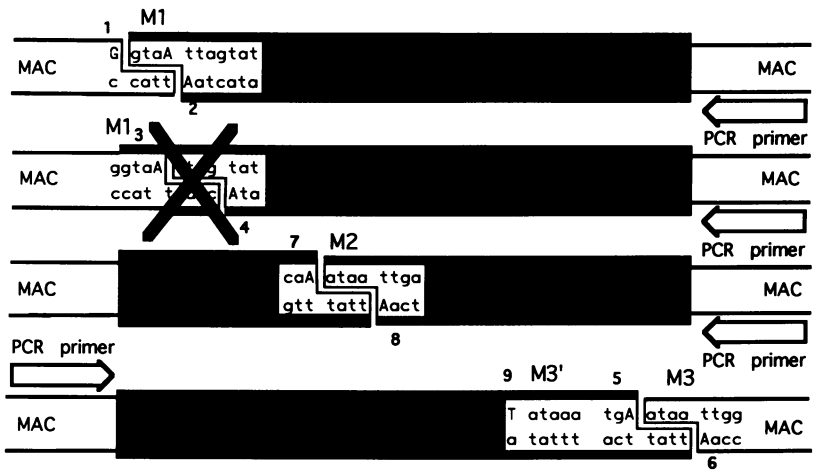

Fig. 9. Map of unique end cleavage sites observed during IES excision in the M region. The black box designates the IES. Arrows denote positions of second PCR primers used to amplify each of the MIC ends shown. Other numbers and designations are as in Figure 3.

in the PCR amplification steps was >1.2 kbp in length. We detected a PCR product corresponding to the initiating break at the R2 deletion boundary only when an additional amplification step was applied (data not shown). Because of extremely low G+C content in the DNA flanking the R region, the amplification primers used in the study of this region contain just 20–25% G and C residues, which might reduce the specificity in amplifying these long DNA segments. For comparison, the primers used to study the initiating breaks in the M region are ~45% in G+C content.

All but one of the macronuclear junctions shown in Figure 3 can be explained by an initiating cleavage on one side of an element, at double-strand break sites defined above. The liberated 3′ hydroxyl group (on the MAC side

of the break) would then directly attack a phosphodiester bond on the opposite end of the deleted element to generate the macronuclear junction on one strand. In this way, junction 1 in the R region is generated by an initiating break at R1, while junction 2 would require an initiating break at R2. For the 0.6 kbp deletion in the M region, junction 1 could arise from an initiating cleavage at either M2 or M3 (the 4 bp overlap region is identical on both sides of the deleted element in this case), while junction 2 would arise from cleavage at M2 followed by transesterification at M3′. For the 0.9 kbp deletion in the M region, junctions 1 and 3 can be generated with an initiating cleavage at M3, followed by transesterification at the M1 locations defined by strand breaks 2 and 4, respectively. The lone exception involves junction 2 for the 0.9 kbp deletion. This junction would require cleavage at M1 at the sites corresponding to strand breaks 3 and 4. A double-strand break is detected at this location, but is not detected when the protocol is modified to detect 'initiating' breaks. As noted above, an initiating break is detected 4 bp to the left of this position which does not correspond to any observed macronuclear junction.

We further explored the results at M1. To generate junction 2 for the 0.9 kbp deletion, the DNA strands must be linked at the positions defined by strand breaks 3 and 5. A free and nucleophilic 3′ hydroxyl could be positioned at the point defined by break 3 if the initiating break were generated at strand breaks 1 and 2 (as observed), followed by a filling in of the four nucleotide 5′ extension to generate a blunt end corresponding to the points defined by breaks 3 and 2. We therefore set out to detect blunt-ended DNA at this position, and extended the study to other double-strand break sites described above. The protocol to detect blunt ends did not produce a signal above the non-specific background for most deletion boundaries. A strong specific signal appeared only on the MAC side of the break at the M1 boundary (Figure 10, lanes labeled 1). The signal was again detected only in cells undergoing DNA rearrangement. The sequencing of the PCR product showed that the blunt end appears at the position defined by the breaks 2 and 3. No reciprocal blunt end (above background) was found on the MIC DNA side at this boundary (Figure 10, lanes 2) in five separate trials. Thus, the detected blunt end does not seem to result directly from a flush cut, but is likely to be generated as a result of filling in of the staggered open end generated by cutting at the sites defined by strand breaks 1 and 2.

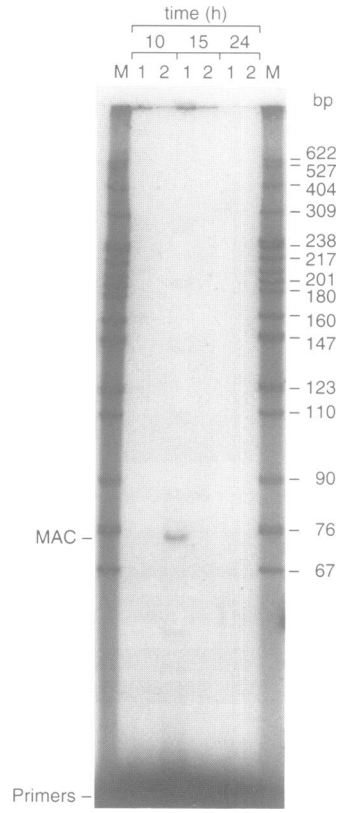

Fig. 10. One open MAC end generated during IES excision at the M1 boundary exists transiently as a blunt end. A ligation-mediated PCR protocol with a blunt-ended linker was used to detect blunt ends at the IES boundaries as described in Materials and methods. Analysis of the MAC and MIC DNA ends at the M1 boundary are shown (lanes 1 and 2, respectively). The cells were analyzed at different times after initiation of conjugation. The molecular size markers (lanes M) are pBR322 fragments generated by *Msp*I digestion. The signal for the MAC end at M1 shown was the only one detected reproducibly with this protocol.

Discussion

There are two general pathways that might explain results obtained to date for the deletion of *Tetrahymena* IES elements like the M and R regions. Deletion might be initiated by cleaving both ends of the element followed by a processing and ligation of the MAC ends. Alternatively, cleavage could occur on only one side of the element, with the macronuclear junction being generated by a direct attack of the liberated 3′ hydroxyl on a phosphodiester bond at the opposite side of the element as outlined in Figure 11. The weight of evidence gathered to date favors the second alternative, with a few caveats discussed below. Much of the evidence has been obtained with PCR-based methods. Several features of the data help to rule out PCR artifacts, including an extensive set of controls along with the evident reproducibility and internal consistency of information obtained with many different protocols. The data is also rationalized readily in the context of the known properties of the M and R region deletions derived from more than a decade of research in the Yao laboratory. The results of the present study provide evidence for the proposed initiation and transesterification steps. At this point, there is little information about the steps needed to process the other strand and release the deleted DNA.

DNA cleavage to initiate M and R region deletion

We have detected double-strand breaks with a location, structure and time of appearance that implicate them as true intermediates in the deletion reaction. The breaks occur precisely at the boundaries of IES elements deleted during macronuclear development in *T.thermophila*. The molecular structure of the breaks is defined completely, and the structure of the DNA ends on the MIC and MAC sides of the breaks are in all cases complementary. All breaks have free 3′ hydroxyl groups and 5′ phosphates, indicating that they are generated by hydrolytic cleavage. Breaks are staggered on the two DNA strands producing ends with four nucleotide 5′ extensions. In 11 of 12 cases,

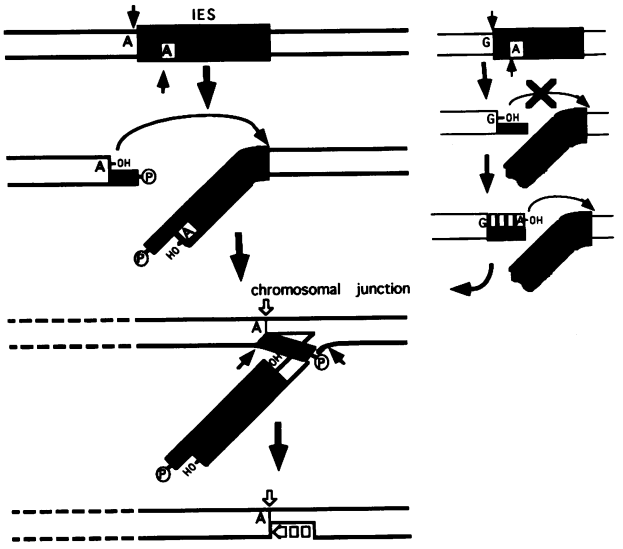

Fig. 11. A model for developmentally programmed deletion at the M and R regions. The reaction is initiated by a single double-stranded DNA cleavage at one boundary of the IES. For most M and R region deletions, the initiating cleavage is directed by adenosine residues arranged as shown in Figure 3, and by other *cis*-acting elements such as the M region G_5 signal defined by the Yao laboratory (Godiska *et al.*, 1993). The cleavage liberates the free 3′ hydroxyl of an adenosine residue on the MAC side of the cleavage which serves as the nucleophile in a transesterification step at a phosphodiester bond at the opposite boundary. The transesterification step creates the macronuclear junction on one DNA strand. The other strand is then processed to generate the mature chromosomal junction by an unspecified pathway (steps implied are entirely speculative). At one M region boundary, a variant pathway is initiated by double-stranded cleavage that leaves a guanosine as the 3′ MAC residue (the minor pathway shown at right). The 3′ hydroxyl liberated as a result of the cleavage is neglected by the splicing machinery. The 3′ adenosine residue required for transesterification is inserted by filling in the DNA end using the 4 bp 5′ extension as template. Subsequent steps are the same as those in the major pathway. Closed arrows indicate cleavage, and open arrows indicate a macronuclear junction.

the 3′-terminal residue at a break is an adenosine. The arrangement of adenosine residues in opposite DNA strands, staggered as shown at the bottom of Figure 4, is likely to represent one of the *cis*-acting signals that specifies the location of DNA cleavage to initiate the deletion reaction. The breaks appear only during the period in which DNA deletion is known to occur during conjugation.

There are two pieces of evidence that a double-strand break is generated on only one side of the element to initiate deletion. First, the macronuclear junction 2 observed for the 0.6 kbp deletion in the M region has an endpoint at a site (M3′) where no double-strand breaks can be detected. The results argue that junction 2 (M, 0.6) is generated by cleavage at M2, followed by direct attack of the liberated 3′ hydroxyl on the appropriate phosphodiester bond at M3′. Second, we can detect double-strand breaks on one end of the deleted sequences in the M region using a protocol (Figure 8A) that requires the other end to be intact. At a minimum, this indicates that simultaneous cleavage at both ends of an element is not obligate. Although we believe that the relative difficulty in detecting initiating breaks in region R by this protocol reflects technical limitations, we cannot eliminate completely the possibility that both ends of the R region are cleaved simultaneously in a deletion pathway that is somewhat distinct from that of region M.

The transesterification step

Although no double-strand breaks were detected at M3′, transesterification at M3′ to generate macronuclear junction 2 (M, 0.6) would liberate a free 3′ hydroxyl on the MIC side of M3′. This 3′ hydroxyl is the only free end we can detect at M3′ with the many different protocols applied to detect and characterize ends, and provides perhaps the best evidence for a transesterification step. Since initiating cleavage events cannot be detected at M3′, the MIC 3′ end observed at this location may provide an opportunity to follow the fate of deleted MIC DNA in later reaction stages without background contributed by competing processes.

Potential variation in the general deletion pathway

The results obtained at boundary M1 for the M region 0.9 kbp deletion are unusual in that they suggest a processing step prior to transesterification. After the break is generated at the locations of strand breaks 1 and 2, the 5′ extension appears to be filled in to generate a blunt end (Figure 11). Transesterification then yields junction 2 (M, 0.9). We could not detect a reproducible generation of blunt ends at any other location, and cannot explain why a fill-in step would occur uniquely at M1. One possibility is that transesterification requires the 3′ hydroxyl of an adenosine residue. The cleavage detected on the MAC side at M1 is the only one that generates a 3′ end with guanosine as the terminal residue. Filling in the 5′ extension inserts an adenosine residue at the 3′ terminus. An adenosine residue appears at all of the identified macronuclear junctions for M and R region deletions. At present, there is insufficient data to determine if this is a general theme for IES deletion reactions in *Tetrahymena*.

We note that deletion to generate the same junction 2 (M, 0.9) could also be initiated by cleavage at the locations of M1 strand breaks 3 and 4, followed by transesterification. This would yield directly the same 3′-terminal adenosine residue as does cleavage at strand break sites 1 and 2 followed by a fill-in of the sticky end. We detect a double-strand break at the location of breaks 3 and 4 (Figure 6), but not an 'initiating' break when the protocol of Figure 8A is used (see Figure 9). This leaves a detected and characterized double-strand break that is associated temporally with the deletion reactions in macronuclear development, but which has no assigned mechanistic role. The function of this double-strand break becomes a question that must be left for future work.

Relationship of M/R region deletions to similar processes in other ciliates

Recent sequence analysis of IES elements in several organisms supports a hypothesis that the elements are copies of ancient transposons (Klobutcher and Herrick, 1995). While IES elements in *T.thermophila* exhibit sequence structures that are among the least transposon-like of ciliate IES elements, the proposed excision pathway for the M and R regions (Figure 11) features cleavage and transesterification steps that suggest a transposon origin. The pathway is also similar to that proposed for

deletion of TBE1 elements in *O.trifallax* (Williams *et al.*, 1993). Further definition of the deletion pathway for the M and R regions, coupled to analysis of other IES elements in *Tetrahymena*, should help elucidate the origin and function of the elements and their relationship to deleted elements in other ciliates.

Materials and methods

Strains and culture conditions

Tetrahymena thermophila strains were CU427.2VI and CU428.1VII, obtained from Peter Bruns, Cornell University (Ithaca, NY). Cell cultivation and mating were carried out as described previously (Bruns and Brussard, 1974). Mating efficiency was not less than 80–90%, as determined by microscopy.

Preparation of cell lysate

Cell lysate was prepared essentially as described previously (Saveliev and Cox, 1995). In short, cells in 50 ml of cell culture were collected by centrifugation and lysed in 10 ml of SDS-pronase buffer [1% SDS, 0.5 M EDTA, 10 mM Tris–HCl (final pH 9.5), 0.2 mg/ml pronase (Austerberry and Yao, 1987)] at 60°C for 4 h. The lysate was then dialyzed at room temperature for several hours. The dialysis was continued in fresh TE at 4°C overnight. Preliminary experiments showed that the enzymes used to label DNA ends in the current study are largely or completely inhibited by an unknown component of lysates prepared in this way. Further purification of the lysate was provided by extraction with 3 vol of chloroform:isoamyl ethanol. The mixture was agitated slowly and gently to minimize DNA breakage. After several minutes of extraction, the aqueous and chloroform phases were separated by microcentrifugation for 1 min. The upper phase (DNA solution) was transferred gently to a new dialysis bag. As described previously (Saveliev and Cox, 1995), the 1 ml plastic pipet tip used for the transfer was cut to widen the opening and minimize DNA shearing. The lysate was again dialyzed at 4°C overnight against 5 mM Tris–HCl buffer, pH 6.8 to remove the remaining chloroform. This dialyzed lysate was used in the procedures described below.

The DNA concentration was estimated by ethidium bromide fluorescent quantitation analysis in a 0.75% agarose gel containing 1 μg/ml of ethidium bromide (Sambrook *et al.*, 1989).

Analysis of 3′ ends

3′ DNA end extension. A 500 μl aliquot of the lysate (1–1.2 μg of genomic DNA) was transferred from the dialysis bag to a 1.5 ml microcentrifuge tube. As described above, a cut 1 ml micropipet tip was used for the transfer. DNA was denatured at 94°C for 3 min to expose free 3′ DNA ends in the solution. The denatured lysate was placed in ice, and 125 μl of buffer A [500 mM cacodylate buffer, (pH 6.8); 5 mM $CoCl_2$; 0.5 mM dithiothreitol (DTT); 500 μg/ml bovine serum albumin (BSA); 80 μM dGTP; 1 U/μl of TdT (Promega)] was added. Mixing was provided by several gentle inversions of the tube. The tailing reaction was carried out at 37°C for 45 min. DNA was then precipitated by 3 volumes of ethanol in the presence of 2 M ammonium acetate and 100 μg/ml of glycogen at –70°C for 2 h.

3′ DNA end amplification. The precipitate obtained in the previous step was collected by microcentrifugation for 15 min at 4°C, and redissolved in 300 μl of buffer B [2 mM Tris–HCl (pH 8.0) 0.2 mM EDTA]. A 30 μl aliquot (containing ~100 ng of genomic DNA) was used for an individual analysis. This aliquot was transferred to a 0.5 ml PCR tube and mixed with 20 μl of buffer C [0.5 mM of each dGTP, dATP, dTTP and dCTP; 6.25 mM $MgCl_2$; 125 mM KCl; 25 mM Tris–HCl (pH 9.0); 0.25% Triton X-100; 25% glycerol; 0.2 μM oligonucleotide A(C)]. The mixture was covered with a layer of mineral oil, incubated at 94°C for 3 min and annealed at 50°C for 30 min. Then 2 μl of a 10 μM solution of oligonucleotide A, 2 μl of a 10 μM solution of the appropriate first amplification primer and 0.4 μl of *Taq* DNA polymerase (5 U/μl) were added directly to the 50°C solution. After continuing the incubation at 50°C for several seconds, the mixture was brought to 72°C and incubated at this temperature for 3 min to extend the annealed dC tail of the anchor oligonucleotide A(C). The mixture then immediately proceeded into 35 PCR cycles for amplification. Each cycle consisted of 1 min at 94°C, 1 min at 55°C (or 62°C for some amplification primers) and 3 min at 72°C. Cycling was concluded with a final extension at 72°C for 7 min.

If required, an additional amplification was carried out. The PCR products obtained after the first amplification were diluted 20- to 2000-fold (exact dilution determined empirically). The PCR mixture contained 0.4 μM each of anchor oligonucleotide A [or, in some reactions, A(C)] and the appropriate second (nested) amplification primer; 0.2 mM each of dGTP, dATP, dTTP and dCTP; 2.5 mM $MgCl_2$; 50 mM KCl; 10 mM Tris–HCl (pH 9.0); 0.1% Triton X-100; 10% glycerol and 0.4 μl of *Taq* DNA polymerase (5 U/μl) (Promega) in 50 μl total volume. The mixture was covered with a layer of mineral oil and transferred into the pre-heated cycler at 94°C. After incubation at this temperature for 3 min, amplification was carried out by PCR for 35 cycles as above.

Analysis of double-strand breaks

Linker ligation to open chromosomal ends. An 18 μl aliquot of dialyzed cell lysate (containing ~50 ng of genomic DNA) was transferred gently to a 0.5 ml PCR tube. All the precautions used to minimize DNA breakage were as in the 3′ end detection procedure above. To the lysate was added 2 μl of buffer D [0.3 M Tris–HCl (pH 7.7); 0.1 M $MgCl_2$; 0.1 M DTT; 10 mM ATP; 2 μM staggered anchor linker or 10 μM blunt-ended anchor linker as appropriate; and 0.1 or 0.5 Weiss units/μl of T4 DNA ligase (depending upon whether the staggered linker or the blunt-ended linker was to be ligated, respectively)]. The ligation was carried out at 16°C overnight.

Amplification of open chromosomal ends. A 5 μl aliquot of the ligated mixture (containing ~15 ng of genomic DNA) was mixed with 45 μl of PCR buffer [0.45 μM each of anchor oligonucleotide I and the appropriate amplification primer; 0.22 mM each of dGTP, dATP, dTTP and dCTP; 2.78 mM $MgCl_2$; 0.055 M KCl; 0.011 M Tris–HCl (pH 9.0); 0.11% Triton X-100; 11% glycerol]. The mixture was incubated at 94°C for 3 min and 55°C for 3 min, followed by addition of 0.4 μl of *Taq* DNA polymerase (5 U/μl) (Promega). The mixture was covered with a layer of mineral oil and PCR amplification was carried out for 35 cycles as described above except that the extension step in each cycle was 1 min.

Analysis of amplification products

The PCR products obtained in each procedure were precipitated with 3 volumes of ethanol in the presence of 2 M ammonium acetate and 100 μg/ml of glycogen at –70°C for 2 h. The precipitate was resuspended in 20 μl of extension buffer [40 pmol/ml visualization primer end-labeled with [γ-^{32}P]ATP; 0.2 mM each of dGTP, dATP, dTTP and dCTP; 2.5 mM $MgCl_2$; 50 mM KCl; 10 mM Tris–HCl (pH 9.0); 0.1% Triton X-100; 40 U/ml of *Taq* DNA polymerase]. The mixture was incubated for 3 min at 94°C, 1 min at 55°C and 7 min at 72°C. A portion of the mixture (5 μl) was mixed with 3 μl of sequencing stop solution (Sambrook *et al.* 1989) and analyzed by electrophoresis in 6% PAGE under denaturing conditions. After electrophoresis, the extended products were visualized by exposure of the gel with X-ray film.

Direct sequencing of PCR products

Isolation, reamplification and sequencing of PCR products were carried out as described previously (Saveliev and Cox, 1995). Minor variations were introduced for the analysis of the PCR products obtained in the 3′ DNA end detection procedure. In particular, the extension time during reamplification of the PCR products was 3 min and the primer used for sequencing was the appropriate ^{32}P-end-labeled vis primer listed below.

PCR primers and anchor linkers

Oligonucleotides used as PCR primers in the 3′ end analysis are as follows: R1MACfirst, 5′-ACCAAATGTATGTATTTATGTATACTC-TAA-3′; R1MACsecond, 5′-TACTAAATTATTCTTTATAATCTGACT-CTT-3′; R1MACvis, 5′-CCAAAAAGCTAATTAAAAATCAAAATC-TATAAATC-3′; R1MICfirst, 5′-TGCTTAGAGTATCTTATTAATGAG-ATATTG-3′; R1MICsecond, 5′-CCTCAATTTACCTCATGTTGGCTA-TCT-3′; R1MICvis, 5′-CGGAAATACTTCGTTCATATTTATTTGTAT-3′; R2MACfirst, 5′-CGCATTAGTTTATAATCTCTTACCAAGTT-3′; R2MACsecond, 5′-GATTTACTGTAAGATAGTTCTAGAATAAGAC-3′; R2MACvis, 5′-GACAAAAATATTTTTGAAAAATAATTTTTTCA-TTC-3′; R2MICfirst, 5′-GTACTCCACAATATTCATAAATATTAGT-CACTG-3′; R2MICsecond, 5′-CAAGACTAAATGTTTGATATATTT-CTAACTC-3′; R2MICvis, 5′-TAATTCACGTAATCAAGGACTACTA-ATATT-3′; M1MACfirst, 5′-GCCATATTGAGTTGTTTATTCTGAAAT-TTATCC-3′; M1MACvis, 5′-GTAAATAATAAGGAACCTCTTACTG-TGATA-3′; M1MICfirst, 5′-GGAGATTTTCTTTAAGTCAAGGATGG-AAAC-3′; M1MICsecond, 5′-CTCTATCTATACAAACACAGTTGAT-GGT-3′; M1MICvis, 5′-TGATGGTATTTTAATTTCAGGATTAGCAAT-3′; M2MACfirst, 5′-ATACCATCAACTGTGTTTGTATAGATAGAG-3′; M2MACsecond, 5′-TTGATGCCTTTTCTAATATTTTCAACTT-3′; M2-

MACvis, 5′-TTTCCATCCTTGACTTAAAGAAAATCTCC-3′; M2MICfirst, 5′-ATCTACGACAACCTATTGTACCACAC-3′; M2MICsecond, 5′-TATCAGTTCTCATCAAGTTGTAATGCTA-3′; M2MICvis, 5′-TTTAGAGAGGCTGGTCTCCTTATTCA-3′; M3MACfirst, 5′-GTTTAAAATAAGACTAATCTATAAATAAGG-3′; M3MACsecond, 5′-GAGGGAGAAGGATTCAACAAAGTAAGC-3′; M3MACvis, 5′-TTCAACAAAGTAAGCAAAATTTAACC-3′; M3MACvis2, 5′-GCAAAATTTAACCAATTATTCATTCAT-3′; M3MICfirst, 5′-AAAGCAAGAAGGCTACTTAGCTTTCAAATT-3′; M3MICvis, 5′-GCATTAATCACAATTTTGTTTCGGATTTTC-3′.

In the 3′ DNA end detection procedure, oligonucleotides with the designation first, second and vis were used for the first PCR amplification, the second PCR amplification (where needed) and the visualization step, respectively. The oligonucleotides with the designation MAC were used to study the 3′ ends of the macronucleus-retained chromosomal DNA and those with the designation MIC were used to study the 3′ ends of the micronucleus-specific deleted DNA. The designations R1, M1, etc., refer to the deletion endpoints (shown in Figure 1) that a given set of oligonucleotides was used to analyze.

The anchor oligonucleotide A(C) used in the annealing-extension step of the 3′ detection procedure was 5′-GATCTCATGCTGGAGTTCTTCGCCAAGT$(C)_{16}$-3′, and the anchor oligonucleotide A used as a primer in the PCR amplification step of the same procedure was 5′-GATCTCATGCTGGAGTTCTTCGCC-3′.

In the procedure to detect double-stranded breaks, the primers used in the amplification step and the visualization step were the oligonucleotides above with the designations second and vis, respectively. Again, the oligonucleotides with the designation MAC were used to detect the open ends of the macronucleus-retained chromosomal DNA and those with the designation MIC were used to detect the open ends of the deleted DNA. The designations R1, M1, etc., are as above.

The anchor linker used to study the blunt-ended open chromosomal ends was prepared by annealing the I and J oligonucleotides described previously (Saveliev and Cox, 1995). The anchor linkers used to study the staggered-ended double-strand breaks were prepared by annealing the I oligonucleotide with an oligonucleotide equivalent to J but lengthened by four or five nucleotides as shown below. Only the 5′ variable ends are shown for the J-derived oligonucleotides. Oligonucleotides with four nucleotide extensions are: JM2MIC or JM3MAC, 5′-TTAT.....-3′; JM2MAC or JM3MIC, 5′-ATAA.....-3′; JM1 (3/4)MIC, 5′-CTAA.....-3′; JM1 (3/4)MAC, 5′-TTAG.....-3′; JR1MIC, 5′-TCAC.....-3′; JR1MAC, 5′-GTGA.....-3′; JR2MIC, 5′-ACAA.....-3′; JR2MAC, 5′-TTGT.....-3′; JM1 (1/2)MAC, 5′-GTAA.....-3′; and JM1 (1/2)MIC, 5′-TTAC.....-3′. Oligonucleotides with five nucleotide extensions are: JM2MIC5 or JM3MAC5, 5′-TTATT.....-3′; JM2MAC5 or JM3MIC5, 5′-ATAAT.....-3′; JM1 (3/4)MAC5, 5′-TTAGT.....-3′; JR1MAC5, 5′-GTGAT.....-3′; JR1MIC5, 5′-TCACT.....-3′; JR2MIC5, 5′-ACAAT.....-3′; JR2MAC5, 5′-TTGTT.....-3′. The J-derived oligonucleotides with the designation MAC and MIC were used to construct the linkers, which are compatible with open ends of the macronucleus-retained chromosomal DNA and the deleted DNA, respectively. R1, M1, etc., designate the deletion endpoints that a given oligonucleotide was used to analyze. M1 1/2 and M1 3/4 designate the two alternative sets of DNA breaks in the M1 deletion endpoint.

All the oligonucleotides used in the study were gel-purified (Sambrook *et al.*, 1989).

Acknowledgements

This work was supported in part by grant 135-0520 from the University of Wisconsin Graduate School.

References

Austerberry,C.F. and Yao,M.C. (1987) Nucleotide sequence structure and consistency of a developmentally regulated DNA deletion in *Tetrahymena thermophila*. *Mol. Cell. Biol.*, **7**, 435–443.

Austerberry,C.F. and Yao,M.C. (1988) Sequence structures of two developmentally regulated, alternative DNA deletion junctions in *Tetrahymena thermophila*. *Mol. Cell. Biol.*, **8**, 3947–3950.

Austerberry,C.F., Allis,C.D. and Yao,M.C. (1984) Specific DNA rearrangements in synchronously developing nuclei of *Tetrahymena*. *Proc. Natl Acad. Sci. USA*, **81**, 7383–7387.

Austerberry,C.F., Snyder,R.O. and Yao,M.C. (1989) Sequence microheterogeneity is generated at junctions of programmed DNA deletions in *Tetrahymena thermophila*. *Nucleic Acids Res.*, **17**, 7263–7272.

Blackburn,E.H. (1992) Telomerases. *Annu. Rev. Biochem.*, **61**, 113–129.

Bruns,P.J. and Brussard,T.B. (1974) Pair formation in *Tetrahymena pyriformis*, an inducible developmental system. *J. Exp. Zool.*, **188**, 337–344.

Cherry,J.M. and Blackburn,E.H. (1985) The internally located telomeric sequences in the germ-line chromosomes of *Tetrahymena* are at the ends of transposon-like elements. *Cell*, **43**, 747–758.

Craig,N.L. (1988) The mechanism of conservative site-specific recombination. *Annu. Rev. Genet.*, **22**, 77–105.

Deng,G. and Wu,R. (1983) Terminal transferase: use of the tailing of DNA and for *in vitro* mutagenesis. *Methods Enzymol.*, **100**, 96–116.

Doak,T.G., Doerder,F.P., Jahn,C.L. and Herrick,G. (1994) A proposed superfamily of transposase genes: transposon-like elements in ciliated protozoa and a common 'D35E' motif. *Proc. Natl Acad. Sci. USA*, **91**, 942–946.

Godiska,R. and Yao,M.C. (1990) A programmed site-specific DNA rearrangement in *Tetrahymena thermophila* requires flanking polypurine tracts. *Cell*, **61**, 1237–1246.

Godiska,R., James,C. and Yao,M.C. (1993) A distant 10-bp sequence specifies the boundaries of a programmed DNA deletion in *Tetrahymena*. *Genes Dev.*, **7**, 2357–2365.

Heinonen,T.Y. and Pearlman,R.E. (1994) A germ line-specific sequence element in an intron in *Tetrahymena thermophila*. *J. Biol. Chem.*, **269**, 17428–17433.

Jaraczewski,J.W. and Jahn,C.L. (1993) Elimination of Tec elements involves a novel excision process. *Genes Dev.*, **7**, 95–105.

Katoh,M., Hirono,M., Takemasa,T., Kimura,M. and Watanabe,Y. (1993) A micronucleus-specific sequence exists in the 5′-upstream region of calmodulin gene in *Tetrahymena thermophila*. *Nucleic Acids Res.*, **21**, 2409–2414.

Klobutcher,L.A. and Herrick,G. (1995) Consensus inverted terminal repeat sequence of *Paramecium* IESs: resemblance to termini of Tc1-related and *Euplotes* Tec transposons. *Nucleic Acids Res.*, **23**, 2006–2013.

Klobutcher,L.A., Turner,L.R. and LaPlante,J. (1993) Circular forms of developmentally excised DNA in *Euplotes crassus* have a heteroduplex junction. *Genes Dev.*, **7**, 84–94.

Loh,E.Y., Elliott,J.F., Cwirla,S., Lanier,L.L. and Davis,M.M. (1989) Polymerase chain reaction with single-sided specificity: analysis of T cell receptor delta chain. *Science*, **243**, 217–220.

Madireddi,M.T., Davis,M.C. and Allis,C.D. (1994) Identification of a novel polypeptide involved in the formation of DNA-containing vesicles during macronuclear development in *Tetrahymena*. *Devel. Biol.*, **165**, 418–431.

Martindale,D.W., Allis,C.D. and Bruns,P.J. (1982) Conjugation in *Tetrahymena thermophila*. A temporal analysis of cytological stages. *Exp. Cell Res.*, **140**, 227–236.

Orias,E. (1986) Ciliate conjugation. In Gall,J.G. (ed.), *The Molecular Biology of Ciliated Protozoa*. Academic Press, Orlando, FL, pp. 45–84.

Sambrook,J., Fritsch,E.F. and Maniatis,T. (1989) *Molecular Cloning: A Laboratory Manual*. 2nd edn. Cold Spring Harbor Laboratory Press, Cold Spring Harbor, NY.

Saveliev,S.V. and Cox,M.M. (1994) The fate of deleted DNA produced during programmed genomic deletion events in *Tetrahymena thermophila*. *Nucleic Acids Res.*, **22**, 5695–5701.

Saveliev,S.V. and Cox,M.M. (1995) Transient DNA breaks associated with programmed genomic deletion events in conjugating cells of *Tetrahymena thermophila*. *Genes Dev.*, **9**, 248–255.

Wells,J.M., Ellingson,J.L., Catt,D.M., Berger,P.J. and Karrer,K.M. (1994) A small family of elements with long inverted repeats is located near sites of developmentally regulated DNA rearrangement in *Tetrahymena thermophila*. *Mol. Cell. Biol.*, **14**, 5939–5949.

Williams,K., Doak,T.G. and Herrick,G. (1993) Developmental precise excision of *Oxytricha trifallax* telomere-bearing elements and formation of circles closed by a copy of the flanking target duplication. *EMBO J.*, **12**, 4593–4601.

Yao,M.-C. (1989) Site-specific chromosomal breakage and DNA deletions in ciliates. In Berg,D.E. and Howe,M.M. (eds), *Mobile DNA*. American Society for Microbiology, Washington, DC, pp. 715–734.

Yao,M.C. (1996) Programmed DNA deletions in *Tetrahymena*: mechanisms and implications. *Trends Genet.*, **12**, 26–30.

Yao,M.C. and Yao,C.H. (1994) Detection of circular excised DNA deletion elements in *Tetrahymena thermophila* during development. *Nucleic Acids Res.*, **22**, 5702–5708.

Received on December 4, 1995; revised on February 5, 1996